J. Plasma Physics (2006), *vol.* 72, *part* 6, *pp.* 1057–1060. © 2006 Cambridge University Press
doi:10.1017/S0022377806005228 Printed in the United Kingdom

Comparison of numerical interpolation schemes for one-dimensional electrostatic Vlasov code

TAKAYUKI UMEDA,[1] MAHA ASHOUR-ABDALLA,[1,2] and DAVID SCHRIVER[1]

[1]Solar Terrestrial Environment Laboratory, Nagoya University, Nagoya, Aichi 464 8601, Japan
[2]Department of Physics and Astronomy, University of California, Los Angeles, Los Angeles, CA 90095-1547, USA

(Received 24 July 2005 and accepted 5 December 2005)

Abstract. We discuss numerical interpolation schemes used in Vlasov codes. An improved conservative semi-Lagrangian scheme is compared with the latest non-conservative and conservative schemes for a long run-time nonlinear problem of the beam–plasma interaction with respect to the mass and energy conservation.

1. Introduction

Due to the low noise level, Vlasov codes are widely used to study nonlinear kinetic processes in plasmas. Recent Vlasov codes use conservative or non-conservative semi-Lagrangian interpolation schemes (Cheng and Knorr 1976; Nakamura and Yabe 1999; Filbet et al. 2001; Umeda et al. 2003). Characteristics of the recent codes for classical problems of plasma physics were studied by Filbet and Sonnendrucker (2003). The purpose of this paper is twofold. The first is to develop an improved conservative scheme for solving hyperbolic equations, and the second is to compare the new scheme with the latest non-conservative and conservative schemes by performing one-dimensional Vlasov simulations.

2. Numerical methods

In this study we solve the Vlasov equation with the time-advance algorithm called the 'splitting method' (Cheng and Knorr 1976), in which the Vlasov equation without magnetic fields splits into the following two advection equations:

$$\frac{\partial f_s}{\partial t} + v_x \frac{\partial f_s}{\partial x} = 0, \tag{2.1a}$$

$$\frac{\partial f_s}{\partial t} + \frac{q_s}{m_s} E_x \frac{\partial f_s}{\partial v_x} = 0, \tag{2.1b}$$

where the subscript s represents particle species (e.g. electrons and ions). The time advance of distribution functions $f_s(x, v_x)$ is carried out by shifting the distribution function in the x direction (2.1a) with the time step $\Delta t/2$, computing spatial profiles of charge density ρ by integration the distribution functions over v_x, solving Poisson's equation to obtain spatial profiles of electric field E_x, shifting

https://doi.org/10.1017/S0022377806005228 Published online by Cambridge University Press

the distribution function in the v_x direction (2.1b) with the time step Δt, and again shifting the distribution function in the x direction (2.1a) with the time step $\Delta t/2$.

To solve the above two advection equations, we used the original (cubic) and rational constrained interpolation profile (CIP) schemes which are high-accuracy non-conservative semi-Lagrangian schemes widely used in many fields (Nakamura and Yabe 1999; Yabe et al. 2001), the positive and flux conservative (PFC) scheme which is a third-order conservative semi-Lagrangian scheme (Filbet et al. 2001), and the third-order conservative polynomial interpolation (CPI-3) scheme which is an improved version of the PFC scheme. Note that we used exactly the same numerical procedure described in Nakamura and Yabe (1999) for the CIP-type Vlasov codes. A detailed description of CIP-type schemes is given in Yabe et al. (2001) and references therein, so it should not be repeated here, whereas the numerical procedure of a conservative semi-Lagrangian scheme is briefly reviewed.

A solution to the one-dimensional advection equation $\partial f/\partial t + v\partial f/\partial x = 0$ in a conservative semi-Lagrangian scheme takes the following form

$$f_i^{t+\Delta t} = f_i^t + U_{i-1/2}(\nu) - U_{i+1/2}(\nu), \tag{2.2}$$

where U represents a numerical flux, $\nu = v(\Delta t/\Delta x)$, and v is a constant advection velocity, i.e. v_x and $(q_s/m_s)E_x$ in (2.1a) and (2.1b). It is easy to derive the third-order numerical flux for a positive velocity $\nu > 0$ with the following boundary conditions, $U_{i+1/2}(0) = 0$, $U_{i+1/2}(1) = f_i$, $U_{i+1/2}(-1) = -f_{i+1}$, $U_{i+1/2}(2) = f_i + f_{i-1}$. The third-order numerical flux takes the following cubic polynomial form,

$$U_{i+\frac{1}{2}}(\nu) = \nu\left[f_i + L_i^{(1)}\frac{(1-\nu)(2-\nu)}{6} + L_i^{(2)}\frac{(1-\nu)(1+\nu)}{6}\right] \quad \text{for } v \geqslant 0, \tag{2.3a}$$

$$U_{i+\frac{1}{2}}(\nu) = \nu\left[f_{i+1} + L_{i+1}^{(2)}\frac{(1+\nu)(2+\nu)}{6} + L_{i+1}^{(1)}\frac{(1-\nu)(1+\nu)}{6}\right] \quad \text{for } v < 0, \tag{2.3b}$$

where $L_i^{(1)} = f_{i+1} - f_i$ and $L_i^{(2)} = f_i - f_{i-1}$.

It is well known that profiles interpolated by higher-order polynomials become highly oscillatory. If $\partial U/\partial x$ is monotonic, the scheme becomes a total variational diminishing (TVD) scheme. On the other hand, if the numerical flux $U_{i+1/2}$ is a monotone increasing function, i.e. $\partial U/\partial x \geqslant 0$, the value of f_i becomes positive at all times. To preserve positivity, Filbet et al. (2001) introduced the following flux limiters or slope correctors for the PFC scheme,

$$L_i^{(1)} = \begin{cases} \min[2(f_i - f_{\min}), (f_{i+1} - f_i)] & \text{if } f_{i+1} \geqslant f_i \\ -\min[2(f_{\max} - f_i), (f_i - f_{i+1})] & \text{if } f_{i+1} < f_i \end{cases} \tag{2.4a}$$

$$L_i^{(2)} = \begin{cases} \min[2(f_{\max} - f_i), (f_i - f_{i-1})] & \text{if } f_i \geqslant f_{i-1} \\ -\min[2(f_i - f_{\min}), (f_{i-1} - f_i)] & \text{if } f_i < f_{i-1} \end{cases} \tag{2.4b}$$

with $f_{\max} = f_\infty \equiv \max_{I=1\sim N_x}[f_I]$, $f_{\min} = 0$. However, one can find that the profile becomes oscillatory to have local maximum and/or minimum between f_∞ and 0. A TVD (i.e. monotonic) scheme proposed in this paper uses

$$f_{\max} = \max[f_{i+1}, f_i, f_{i-1}], \quad f_{\min} = \min[f_{i+1}, f_i, f_{i-1}],$$

whereas a non-oscillatory (NO) scheme uses

$$f_{\max} = \max\left[f_{i+1}, f_{i-1}, \min[2f_{i-1} - f_{i-2}, 2f_i - f_{i+1}], \min[2f_i - f_{i-1}, 2f_{i+1} - f_{i+2}]\right],$$
$$f_{\min} = \min\left[f_{i+1}, f_{i-1}, \max[2f_{i-1} - f_{i-2}, 2f_i - f_{i+1}], \max[2f_i - f_{i-1}, 2f_{i+1} - f_{i+2}]\right],$$

https://doi.org/10.1017/S0022377806005228 Published online by Cambridge University Press

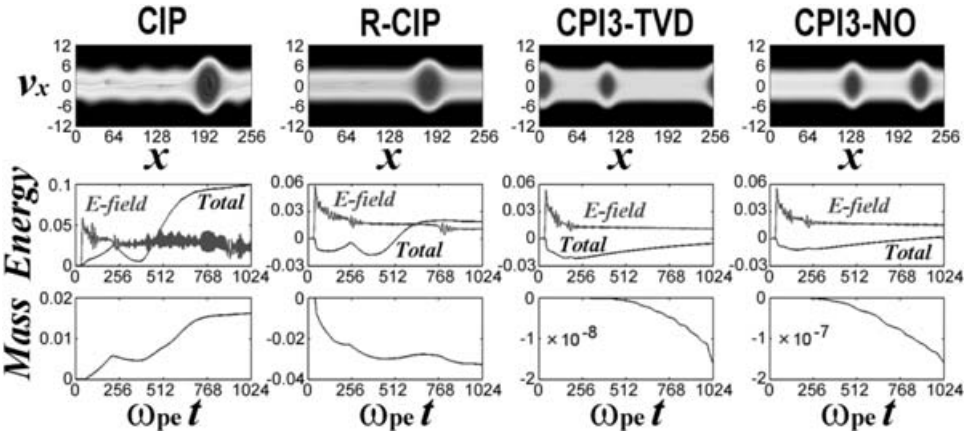


Figure 1. Simulation result: phase-space electron densities $f(x, v)$ at $\omega_{\rm pe}t = 1024$ (top), time histories of total energy $(\mathscr{E}(t) - \mathscr{E}_0)/\mathscr{E}_0$ and electric field energy (middle), time histories of total mass $(\mathscr{M}(t) - \mathscr{M}_0)/\mathscr{M}_0$ (where $\mathscr{M} \equiv \sum_{i,j} |f(x_i, v_j)|$ (bottom)); obtained with original CIP, rational CIP, CPI-3 with TVD limiter and with NO limiter.

to detect the valid maximum or minimum. It is also noted that we can preserve positivity if $f_{\rm min} \geqslant 0$.

3. Vlasov simulations

We have performed simulation runs of the electron two-stream instability to study the characteristics of the different interpolation schemes for a long run-time and a strong nonlinear problem. We assume two electron beams having equal density 0.5 and equal initial thermal velocity $V_{\rm t} = 1.0$. The two electron beams drift along the ambient magnetic field with a drift velocity $V_{\rm d} = \pm 3.0 V_{\rm t}$. The number of cells in the x-direction is $N_x = 256$ and $N_v = 256$ in the v-direction, with $v_{\rm max} = 12V_{\rm t}$, $v_{\rm min} = -12V_{\rm t}$. The grid spacing is equal to $\Delta x = V_{\rm t}/\omega_{\rm pe}$, and the time step is equal to $\omega_{\rm pe}\Delta t = 0.01$. In the x direction we imposed the periodic boundary condition. In the v_x direction we imposed the open boundary condition where constant numerical fluxes $v_{\rm max} f(v_{\rm max})$ and $v_{\rm min} f(v_{\rm min})$ are assumed while outgoing perturbations of distribution functions are perfectly absorbed.

In the top panels of Fig. 1, we plot phase-space electron densities $f(x, v)$ at $\omega_{\rm pe}t = 1024$ obtained with the original CIP scheme, the rational CIP scheme, the CPI-3 scheme with TVD limiter and the CPI-3 scheme with the NO limiter. In the middle panels we plot the corresponding time histories of total energy $\mathscr{E}$ and electric field energy. In the bottom panels we plot the corresponding time histories of total mass $\mathscr{M}$. Here we define the total mass as $\mathscr{M} \equiv \sum_{i,j} |f(x_i, v_j)|$. The energy and mass histories are plotted as deviations from the initial values such that the bottom panels show $(\mathscr{E}(t) - \mathscr{E}_0)/\mathscr{E}_0$, and the middle panels show $(\mathscr{M}(t) - \mathscr{M}_0)/\mathscr{M}_0$, respectively. The electric field energy is normalized by $\mathscr{E}_0$.

For a long run-time nonlinear evolution, the electron two-stream instability develops to form solitary electron phase-space holes. Although we started the test runs with exactly the same initial conditions, the profiles of phase-space distribution functions at $\omega_{\rm pe}t = 1024$ are different from each other. There are spurious oscillations in the distribution function by the original CIP scheme. The CIP scheme can produce apparent overshoot or undershoot which makes a positive gradient in the velocity distribution function. The value of the distribution function can

https://doi.org/10.1017/S0022377806005228 Published online by Cambridge University Press

be negative, and the total mass increases in time as seen in Figure 1. The total energy also increases to excite waves through a non-physical process, i.e. numerical instability caused by the positive gradient in the velocity distribution function. The histories of total energy and mass are similar to each other, which implies that the property of energy conservation is strongly affected by the property of mass conservation. The spurious oscillations in the distribution function can be suppressed by using a rational function. However, the total energy decreases in the early nonlinear stage as the total mass decreases. In the later nonlinear stage, on the other hand, the total energy increases because the distribution becomes wider due to numerical diffusion.

The large deviation in the total mass can be suppressed by using conservative interpolation schemes. The total mass slightly decreases in time because of the open boundary in the v_x direction. The total energies by both TVD and NO conservative schemes decrease through wave–particle interaction because the saturation level of the instability becomes smaller than that by the CIP-type schemes due to higher numerical diffusion as seen in the electric field energy histories. The increase in the total energy for the long-time nonlinear evolution is also due to numerical diffusion. We found that the total energy is conserved better by the NO scheme than by the TVD scheme. The distribution function becomes flat-top/flat-down by using the TVD limiter, because no local maximum or minimum exists in the TVD scheme. The present NO scheme can maintain the maximum and minimum values of the distribution function. The NO scheme provides the best property for the energy conservation, and is more suitable for studies of long-time nonlinear kinetic processes in plasmas.

4. Conclusion

We found that the total energy is conserved better with conservative schemes than with non-conservative schemes. The mass conservation is an important feature and has a direct influence on the energy conservation. In conclusion, NO conservative schemes are more suitable for Vlasov simulations than TVD conservative schemes or non-conservative schemes. A very high-order, positive, conservative, NO but non-TVD scheme is essential for Vlasov simulations.

Acknowledgements

This work was supported by NSF Grant ATM-02-08507 and NASA Grant NNG050GG58G at the University of California, Los Angeles.

References

Cheng, C. Z. and Knorr, G. 1976 The integration of the Vlasov equation in configuration space, *J. Comput. Phys.* **22**, 330–351.

Filbet, F., Sonnendrucker, E. and Bertrand, P. 2001 Conservative numerical schemes for the Vlasov equation, *J. Comput. Phys.* **190**, 501–522.

Filbet, F. and Sonnendrucker, E. 2003 Comparison of Eulerian Vlasov solvers, *Comput. Phys. Commun.* **150**, 247–266.

Nakamura, T. and Yabe, T. 1999 Cubic interpolated propagation scheme for solving the hyper-dimensional Vlasov–Poisson equation in phase space. *Comput. Phys. Commun.* **120**, 122–154.

Umeda, T., Omura, Y., Yoon, P. H., Gaelzer, R. and Matsumoto, H. 2003 Harmonic Langmuir waves. III. Vlasov simulation, *Phys. Plasmas.* **10**, 382–391.

Yabe, T., Xiao, F. and Utsumi, T., 2001 The constrained interpolation profile method for multiphase analysis. *J. Comput. Phys.* **169**, 556–593.

https://doi.org/10.1017/S0022377806005228 Published online by Cambridge University Press